Interference of magneto-intersubband and phonon-induced resistance oscillations in single GaAs quantum wells with two populated subbands

A. A. Bykov and A. V. Goran
Institute of Semiconductor Physics, Siberian Division, Russian Academy of Sciences, Novosibirsk, Russia

S. A. Vitkalov
Physics Department, City College of the City University of New York, New York 10031, USA

(Received 12 January 2010; published 26 April 2010)

Low-temperature electron magnetotransport in single GaAs quantum wells with two populated subbands is studied at large filling factors. Magneto-intersubband (MIS) and acoustic-phonon-induced oscillations of dissipative resistance are found to be coexisting but interfering substantially with each other. The experiments show that amplitude of the MIS oscillations enhances significantly by phonons, indicating "constructive interference" between the electron-phonon scattering and the intersubband electron transitions. Temperature damping of the quantum oscillations is found to be related to broadening of Landau levels caused by considerable electron-electron scattering.

DOI: 10.1103/PhysRevB.81.155322 PACS number(s): 73.43.Qt, 71.70.Di

The magnetotransport phenomena in high-mobility modulation-doped semiconductor structures are commonly studied with only one populated subband (E_1) because the electron mobility decreases with filling second subband (E_2) due to intersubband scattering.[1] The latter also gives rise to, so-called, magneto-intersubband oscillations (MISOs) of the dissipative resistance ρ_{xx}.[2] In electron systems with two populated subbands, MISO have maxima in magnetic fields B satisfying the relation:[3–5] $\Delta_{12}=k\hbar\omega_c$, where $\Delta_{12}=E_2-E_1$ is the energy separation of the subbands, $\omega_c=eB/m^*$ is cyclotron frequency, m^* is effective electron mass, and k is a positive integer. Similarly to well-known Shubnikov-de Haas (SdH) oscillations, MISOs require quantization of the electron spectrum and are periodic in inverse magnetic fields. The electron quantum relaxation time τ_q determines the amplitude of the oscillations.

Another class of magnetoresistance oscillations in semiconductor structures with high electron mobility emerges at elevated temperatures, when acoustic-phonon modes with Fermi momentum become to be populated.[6,7] These oscillations are called phonon-induced resistance oscillations (PIROs). PIROs are result of a modulation of the probability of the electron-phonon scattering with different momentum transfer in quantizing magnetic fields. The dominant phonon-induced scattering between Landau levels changes the direction of the electron motion by 180°, providing $2k_F$ variation in the electron wave vector. The scattering induces the resistance oscillations (PIROs) with period determined by[6] $j=2k_Fu_s/\omega_c$, where u_s is acoustic-phonon velocity and j is positive integer.

In this paper, we show that MISO and PIRO coexist in single GaAs quantum wells with two populated subbands. The coexistence, however, is not a simple sum of these two effects. Our data indicates significant interference between the phonon and the intersubband scattering. The experiment shows that amplitude of the MIS oscillations is enhanced significantly by phonons, indicating a nontrivial effect of the phonon scattering on the linewidth of the intersubband quantum transitions. The effects of temperature on the quantum oscillations are also examined. The oscillations decay at high temperature. The temperature suppression of the oscillations is found to be consistent with the broadening of the quantum electron levels and decrease in the quantum-scattering time $\tau_q(T)$ at high temperatures. The temperature variation in the quantum time is found to be inversely proportional to square of the temperature, indicating leading contribution of the electron-electron interaction to the decrease in the time $\tau_q(T)$ with the temperature.[8,9]

In classically strong magnetic fields, the dissipative resistivity ρ_{xx} can be written as $\rho_{xx}\cong\sigma_{xx}/\sigma_{xy}^2$, where σ_{xx} is dissipative conductivity, $\sigma_{xy}=e^2n_s/m^*\omega_c$ is classical Hall conductivity, and n_s is carrier density. For the presentation of the experimental results following below, we consider the total resistivity ρ_{xx} (and conductivity σ_{xx}) as the sum of independent components coming from different scattering mechanisms. Contributions of the magneto-intersubband scattering and the phonon-induced scattering, which is important at high temperatures,[6–9] are additively included to the total response. The resistance ρ_{xx} can be presented as[10]

$$\rho_{xx}=\rho_{xx}^{(0)}+\rho_{xx}^{(1)}+\rho_{xx}^{(2)}, \tag{1}$$

where $\rho_{xx}^{(0)}$ is quasiclassical resistance, $\rho_{xx}^{(1)}$ is first-order quantum contribution, and $\rho_{xx}^{(2)}$ is second-order quantum contribution. The quasiclassical magnetoresistance reads[11]

$$\rho_{xx}^{(0)}=\rho_0\left[1+r\frac{n_1n_2\mu_1\mu_2(\mu_1-\mu_2)^2B^2}{(n_1\mu_1+n_2\mu_2)^2+(rn_s\mu_1\mu_2)^2B^2}\right], \tag{2}$$

where $\mu_1(n_1)$ and $\mu_2(n_2)$ are electron mobilities (densities) in both subbands, $n_s=n_1+n_2$, and r is dimensionless parameter responsible for intersubband scattering. The SdH oscillations present the first-order quantum contribution while the MISO and PIRO are in the second-order term. The contribution of the MIS oscillations is[5,10]

$$\Delta\rho_{\mathrm{MISO}} = \frac{2m^*\nu_{12}}{e^2 n_s} \times \exp\left[-\frac{\pi}{\omega_c}\left(\frac{1}{\tau_{q1}} + \frac{1}{\tau_{q2}}\right)\right] \times \cos\left(\frac{2\pi\Delta_{12}}{\hbar\omega_c}\right), \tag{3}$$

where ν_{12} is effective intersubband scattering rate. Positive quantum magnetoresistance is another second-order term,[10]

$$\rho_{QUMR} = \frac{2m^*}{e^2 n_s}\left[\frac{n_1}{n_s}\nu_{11} \times \exp\left(-\frac{2\pi}{\omega_c\tau_{q1}}\right) + \frac{n_2}{n_s}\nu_{22} \times \exp\left(-\frac{2\pi}{\omega_c\tau_{q2}}\right)\right], \tag{4}$$

where ν_{11} and ν_{22} are scattering rates in subbands and τ_{q1} and τ_{q2} are quantum relaxation times in subbands.

In the case of two occupied subbands and one acoustic mode with velocity u_s, the phonon-induced oscillations contain four terms corresponding to both the scattering in each of two subbands ($2k_{F1}u_s = j_1\omega_c$ and $2k_{F2}u_s = j_2\omega_c$) and the phonon-induced intersubband scattering [$(k_{F1}+k_{F2})u_s = j_3\omega_c$ and $(k_{F1}-k_{F2})u_s = j_4\omega_c$], where $k_{F1,2}$ is Fermi wave vector in subbands and j_1, j_2, j_3, and j_4 are positive integers. For the phonon-induced resistance oscillations $\Delta\rho_{\mathrm{PIRO}}$, an analytical expression was recently obtained for a single band system. Three periodic components of PIRO, corresponding to the electron resonance scattering on three acoustic modes in GaAs, were identified.[12] The case of the two populated subbands with three acoustic modes has not been analyzed yet. However, it is likely that in this case, the PIRO may contain a sum of 12 periodic components.

We studied symmetrically doped single GaAs quantum wells (width $d_W = 26$ nm) with GaAs/AlAs superlattice barriers[13,14] grown by molecular-beam epitaxy on (100) GaAs substrates. The energy diagram of the quantum wells with two populated subbands is shown in the inset of Fig. 1. Magnetoresistance measurements were performed on 450 $\times 50$ μm Hall bars fabricated using optical lithography and liquid etching. The major part of the measurements was executed in temperature range $T = 4.2-18.4$ K and in magnetic fields $B < 2$ T. The magnetoresistance $\rho_{xx}(B)$ and Hall resistance $\rho_{xy}(B)$ were measured at low-frequency (0.01–1 kHz) current, not exceeding 10^{-6} A. Hall concentration of the electrons $n_H = 8.14 \times 10^{15}$ m^{-2} was obtained from the Hall resistance, measured in magnetic field $B = 0.5$ T. Hall mobility $\mu_H = 119$ m^2/V s was calculated from n_H and the resistance $\rho_{xx}(B=0) = \rho_0$ at $T = 4.2$ K.

Figure 1(a) presents a typical experimental curve of the resistance $\rho_{xx}(B)$ of studied structures at $T = 4.2$ K. The oscillatory part of the resistance consists of two series of SdH oscillations, corresponding to each of the two subbands and being accompanied by MIS oscillations.[2–5] Fourier transform of the resistance plotted vs inverse magnetic fields $\rho_{xx}(1/B)$ (not shown) indicates that in the field range $0.01 < B < 0.5$ T, there are only MIS oscillations with maxima corresponding to $k = \Delta_{12}/\hbar\omega_c$.[15] The subband energy separation obtained from the frequency of the MIS oscillations is $\Delta_{12} = 15.5$ meV. At higher magnetic fields, MIS oscillations

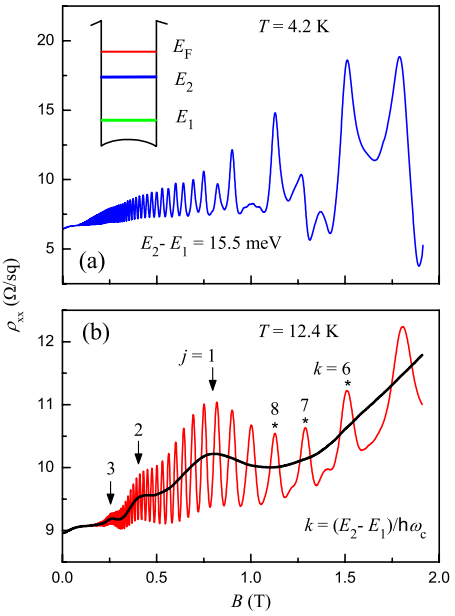

FIG. 1. (Color online) (a) Dependence of resistivity ρ_{xx} on magnetic field B in GaAs quantum well with AlAs/GaAs superlattice barriers at temperature $T = 4.2$ K. Inset presents the energy diagram of the quantum well with energy E_1 and E_2 at bottoms of the two subbands. (b) Dependence of the resistivity ρ_{xx} on magnetic field B at higher temperature $T = 12.4$ K [the gray (red) line]. The low-frequency content of the dependence $\rho_{xx}(B)$ without high-frequency MIS oscillations (the black line). Asterisks mark the maxima of MIS oscillations numbered $k = 6$, 7, and 8. Arrows mark maxima of PIR oscillations numbered $j = 1$, 2, and 3.

coexist with SdH oscillations and the Fourier transform indicates three peaks. Two peaks corresponds to SdH oscillations with frequencies $f_1 \sim E_{F1}$ and $f_2 \sim E_{F2}$ and one peak corresponds to MIS oscillations with frequency $f_{\mathrm{MISO}} \cong f_1 - f_2 \sim E_{F1} - E_{F2} = \Delta_{12}$,[15] where $E_{F1}(E_{F2})$ is Fermi energy, counted from the bottom of first (second) subband. The electron densities n_1 and n_2 in the subbands were calculated, using SdH frequencies f_1 and f_2: $n_1 = 2ef_1/h = 6.24 \times 10^{15}$ m^{-2} and $n_2 = 2ef_2/h = 1.91 \times 10^{15}$ m^{-2}.

Figure 1(b) shows the magnetoresistance at high temperature. At temperature $T = 12.4$ K, SdH oscillations are completely damped due to the temperature broadening of the electron distribution. The amplitude of MISO is also decreased but MISO can still be clearly observed in a wide range of magnetic fields $B > 0.2$ T. In addition to MISO in Fig. 1(b), there is another oscillating component shown by the thick line. These oscillations are absent at temperature $T = 4.2$ K. The asterisks mark the maxima of MISO with $k = 6$, 7, and 8 while the arrows mark three maxima of the new emerging oscillations.

Figure 2 presents the magnetoresistance in broader range of magnetic fields up to 9 T at temperature (a) $T = 4.3$ K and (b) $T = 16$ K. At $T = 16$ K, the Shubnikov-de Haas oscillations are completely damped in magnetic fields up to 9 T due to the temperature broadening of the electron distribution.

Figure 3(a) shows the relative magnetoresistance ρ_{xx}/ρ_0 versus inverse magnetic fields $1/B$ at $T = 12.4$ K. The inset of Fig. 3(b) presents the Fourier transform of the oscillating

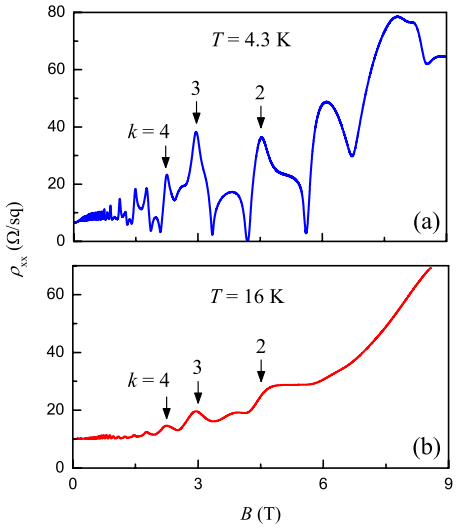

FIG. 2. (Color online) (a) Dependence of resistivity ρ_{xx} on magnetic field B taken in broader range of the field B at temperature T=4.3 K. (b) The magnetic field dependence at T=16 K. At T =16 K, Shubnikov-de Haas oscillations are significantly suppressed in magnetic fields up to 9 T.

part of $\rho_{xx}(1/B)$ measured at T=12.4 K. In the inset, the peak corresponds to MIS oscillations. There are no peaks at the frequencies of SdH oscillations (f_1=12.9 T^{-1} and f_2 =3.95 T^{-1} pointed by arrows in the inset). At T=12.4 K, the

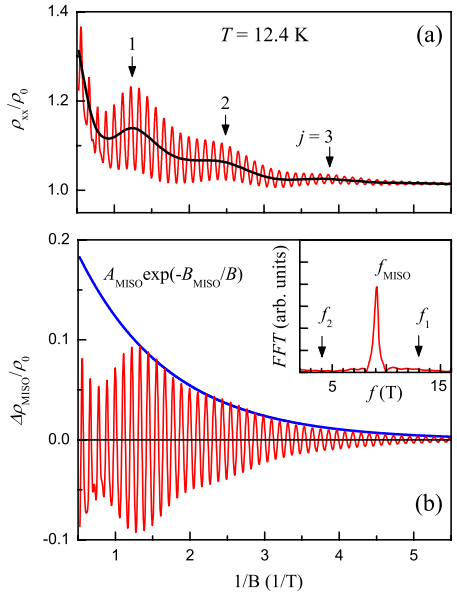

FIG. 3. (Color online) (a) Dependence of relative resistivity ρ_{xx}/ρ_0 on inverse magnetic field $1/B$ at T=12.4 K (the thin line). The thick black line shows the low-frequency content of the dependence $\rho_{xx}(1/B)$ without the high-frequency MIS oscillations. Arrows mark the maxima of PIRO numbered j=1, 2, and 3. (b) Dependence of the MIS oscillations of the resistivity $\Delta\rho_{\mathrm{MISO}}/\rho_0$ on inverse magnetic field $1/B$ (the thin line). The thick line shows expected behavior of the MIS oscillations $A_{\mathrm{MISO}}\exp(-B_{\mathrm{MISO}}/B)$ with A_{MISO}=0.28 and B_{MISO}=0.82 T. Inset presents Fourier transform of the relative resistivity ρ_{xx}/ρ_0 vs $1/B$. Arrows mark the frequencies of SdH oscillations in subbands.

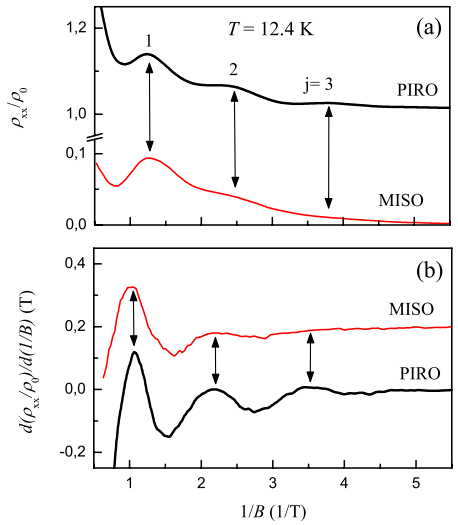

FIG. 4. (Color online) (a) Correlation between PIR oscillations and the amplitude modulation of MIS oscillations in inverse magnetic field. Maximum of PIRO at j=1 corresponds to enhanced amplitude of MISO. (b) First derivative $d\rho_{xx}/d(1/B)$ of the dependences presented in (a), revealing the correlation in broader range of magnetic fields.

contribution of SdH oscillations [the first-order term in Eq. (1)] to the magnetoresistance is negligibly small. Figure 3(b) shows an extracted MISO content, which is difference between the high-frequency oscillations [the gray line in Fig. 3(a)] and the low-frequency background [the black line in Fig. 3(a)]. The amplitude of MISO enhances with increasing magnetic field up to B=0.8 T. An expression $A_{\mathrm{MISO}}\exp(-B_{\mathrm{MISO}}/B)$ with A_{MISO} and B_{MISO} as fitting parameters approximates well the amplitude enhancement at small magnetic fields. The approximation corresponds to theory.[5,10]

At higher magnetic field, however, the amplitude of MIS oscillations does not follow the approximation and deviates considerably from existing theories. At $B>0.8$ T ($1/B<1.25$ T^{-1}), the MISO amplitude decreases by about 50%, which is significantly stronger than few percent variations in the averaged background, shown by the thick black line in Fig. 3(a). Nevertheless, the amplitude modulation of MISO correlates well with the oscillations of the background. This is shown in Fig. 4. In Fig. 4(a), the amplitude modulation of MISO and the background oscillations are plotted together for a comparison. As shown below, the background oscillations correspond to the phonon-induced oscillations of the resistivity (PIRO). A clear correlation between positions of maximums (minimums) of the two sets of oscillations is evident at strong magnetic fields. Figure 4(b) presents fist derivative of the oscillations vs $(1/B)$, revealing the correlation in broader range of magnetic fields. Moreover, the amplitude of PIRO and the amplitude modulations of MISO are comparable suggesting a common origin of these effects.

The modulation of the MISO amplitude with PIRO frequency indicates significant interference between MIS oscillations and PIRO. In accordance with Eq. (3), the amplitude of MIS oscillations depend linearly on rate of the intersubband transport scattering ν_{12} and exponentially on the quantum-scattering time τ_q. Figure 4(a) [see also Fig. 5(b)]

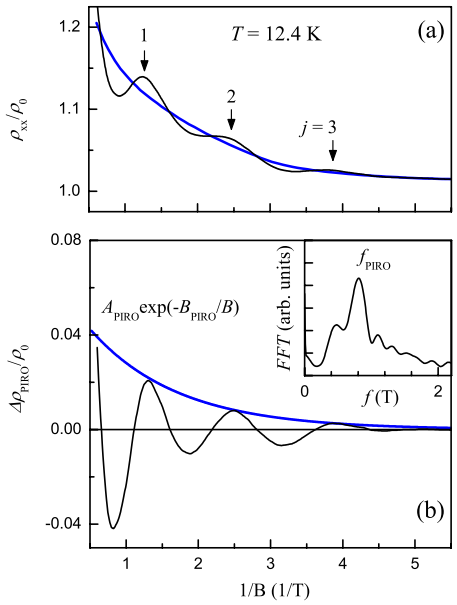

FIG. 5. (Color online) (a) Thin line shows low-frequency content of dependence $\rho_{xx}/\rho_0(1/B)$ without MIS oscillations at temperature $T=12.4$ K. Thick line presents monotonous background of the dependence. Arrows mark the maxima of PIRO numbered $j=1$, 2, and 3. (b) The thin line is difference between two lines presented above in (a). The thin line shows PIR oscillations in inverse magnetic field $\Delta\rho_{\mathrm{PIRO}}/\rho_0(1/B)$. The thick line shows expected behavior of the amplitude of the PIR oscillations in inverse magnetic field $A_{\mathrm{PIRO}}\exp(-B_{\mathrm{PIRO}}/B)$ with $A_{\mathrm{PIRO}}=0.064$ and $B_{\mathrm{PIRO}}=0.82$ T. Inset presents Fourier transform of PIR oscillations $\Delta\rho_{\mathrm{PIRO}}/\rho_0(1/B)$.

demonstrates that phonon-induced variations in the total transport scattering rate $1/\tau_{tr}$ are about 4–6 % at the main PIRO maximum $j=1$. Such small variations in the transport time τ_{tr} cannot account for the 50% reduction in the MISO amplitude at $1/B<1.25$ T^{-1}. This suggests that the phonon-induced variation in the intersubband scattering rate ν_{12}, most likely, is not the dominant mechanism leading to the amplitude modulation of MISO. Since amplitude of quantum oscillations are exponentially sensitive to the quantum-scattering time τ_q, it is likely that the considerable amplitude modulation of MISO with magnetic field is due to variations in the quantum-scattering time τ_q. Due to the correlations with PIRO, the amplitude modulation should be induced by the magneto-oscillations of the electron-phonon scattering (interaction).

It is naturally to assume that an increase in the electron-phonon scattering will decrease the electron quantum-scattering time τ_q, suppressing, in accordance with Eq. (3), the amplitude of MIS oscillations. This, however, is not consistent with the experiment. Figure 4 shows that the suppression of the MISO amplitude occurs at minimums of PIR oscillations, at which the phonon-induced electron scattering appears to be suppressed too and, therefore, the quantum-scattering time τ_q is expected to be long. Thus, instead anticipated "destructive interference" between two processes, the experiments indicates a "constructive interference" between MISO and PIRO. Namely, enhancement of the phonon-induced electron transitions increases the amplitude of the intersubband magneto-oscillations. This indicates a phonon-induced "effective" narrowing of the intersubband resonance in the electron scattering.

The dynamic reduction in resonance linewidth is known phenomenon for the spin resonance.[16] In many cases, the spin-resonance linewidth decreases with increasing temperature. The linewidth reduction is result of an effective averaging of stochastic dipole interactions between spins, when the spins diffuse spatially, exploring more of their phase space. We suggest that a similar physics could be responsible for the apparent decrease in the Landau-level width (increase in the quantum-scattering time τ_q) with the enhancement of the electron-phonon scattering. At high filling factors, the level width is determined by an averaged scattering potential seen by an electron moving along a cyclotron orbit.[17] The electron-phonon scattering enhances the electron diffusion, providing better averaging out of the impurity potential and, thus, reducing the width of Landau levels.

In the subsequent segment of the paper, we present the behavior of the low-frequency oscillations of the resistivity. Figure 5(a) shows the relative magnetoresistance $\rho_{xx}/\rho_0(1/B)$ after removing high-frequency MISO (thin line). The low-frequency content can be further separated into a monotonous component [the thick line in Fig. 5(a)] and a low-frequency oscillating component [the thin line in Fig. 5(b)]. The inset of Fig. 5(b) shows the Fourier transform of the low-frequency oscillations. Assuming that the main peak of the Fourier transform at frequency f_{PIRO} corresponds to the dominant electron-phonon scattering with $q=2k_{F1}$ in the first subband, we obtained the value of $u_s=5.2$ km/s, which is consistent with the velocity of one of the bulk acoustic modes in (100) GaAs layers.[12] Taking also into account that the low-frequency oscillations appear only at high temperatures [another characteristic property of PIRO (Ref. 6)], we identify the low-frequency oscillations as phonon-induced resistance oscillations. It is worth mentioning that the maximums of the PIR oscillations $[j(1/B)]$ are not equally separated from each other. One of the possible reasons for this behavior is that three bulk acoustic modes with different velocities can participate in the resonance scattering. Another possible reason is that in system with two populated subbands both intrasubbbands and intersubbands phonon-induced transitions should contribute to the resistivity.

Figure 6(a) shows magnetoresistance $\rho_{xx}(1/B)$ after removing high-frequency MISO for temperatures in range 8.4–18.4 K. The first oscillation $(j=1)$ is clearly seen for all temperatures while the second and third oscillations $(j=2,3)$ disappear with increasing temperature. Figure 6(b) shows the temperature dependence of the PIRO amplitude $\Delta\rho_{\mathrm{PIRO}}(T)$. The dependence demonstrates maxima at $T_0=12.4$ K for $j=1$ and $T_0=8.6$ K for $j=2$, which is consistent with previous results.[8,9] The temperature dependence of $\Delta\rho_{\mathrm{PIRO}}(T)$ for $j=3$ cannot be extracted with a decent precision. In Fig. 6(b), the solid lines were calculated, using an approximation of the temperature dependence of the PIRO amplitude,[8]

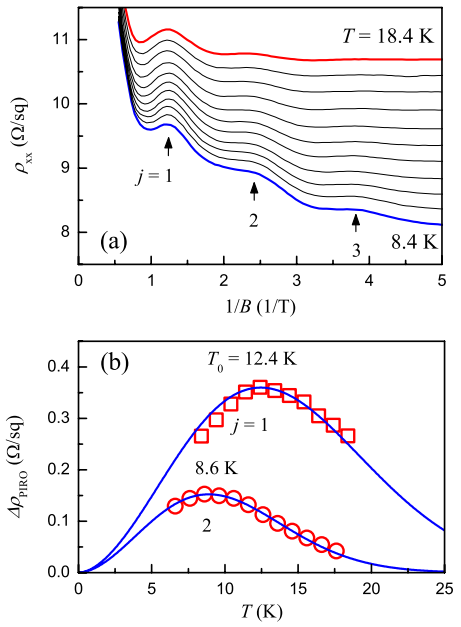

FIG. 6. (Color online) (a) PIR oscillations of resitivity $\rho_{xx}(1/B)$ (MIS oscillations are removed) at different temperatures in range $8.4<T<18.4$ K. Arrows mark the maxima of PIRO numbered $j=1$, 2, and 3. (b) Temperature dependence of amplitude of PIR oscillations $\Delta\rho_{\mathrm{PIRO}}(T)$ for $j=1$ and 2. Symbols present experimental data, extracted from Fig. 6(a). Solid lines are calculated using Eq. (5).

$$\Delta\rho_{\mathrm{PIRO}}(T) \propto \tau_{ph}^{-1}(T)\exp\{-2\pi/[\omega_c\tau_q^{ee}(T)]\}, \qquad (5)$$

where τ_{ph} is an effective electron-phonon scattering time and τ_q^{ee} is a contribution of e-e scattering to the electron quantum lifetime. The term $\tau_{ph}^{-1}(T)$ is responsible for the rise of PIRO amplitude with increasing temperature whereas the term $\exp(-2\pi/\omega_c\tau_q^{ee})$ provides the damping of the oscillations at high temperatures. Assuming that $1/\tau_{ph}(T)\propto T^{\alpha}$ (Refs. 18–20) and $1/\tau_q^{ee}(T)=\lambda T^2/E_F$,[21,22] the amplitude of PIR oscillations $\Delta\rho_{\mathrm{PIRO}}(T)$ can be calculated with two fitting parameters α and λ.[8] In the calculations, we used the value of $\alpha=1.8$ (Ref. 8) and $E_F=E_{F1}$. Figure 6(b) shows a good agreement between experimental and theoretical curves for $\lambda=3.8$.

Figure 7 presents experimental and calculated dependences of the relative resistance $\rho_{xx}/\rho_0(B)$ at $T=12.4$ K. The calculated $\rho_{xx}/\rho_0(B)$ is the sum of contributions of different scattering mechanisms, described by Eqs. (2)–(4) and the electron-phonon resonance scattering. A good agreement with experimental data is obtained in a broad range of magnetic fields for the following fitting parameters: $\mu_1=88.4$ m^2/V s, $\mu_2=76.6$ m^2/V s, and $r=0.25$. The considerable value of r indicates the importance of the intersubband scattering in the studied system. The values of μ_1 and μ_2 are found to be close to each other and to the average mobility $\mu_0=1/e\rho_0 n_s$ with an accuracy of 10%. Neglecting the difference of the quantum-scattering rates in subbands, the magnetoresistance in Eq. (4) was approximated as $\rho_{QUMR}/\rho_0=A_{QUMR}\exp(-B_{QUMR}/B)$, where A_{QUMR} and B_{QUMR} are fitting parameters. The MIS oscillations and PIR oscillations

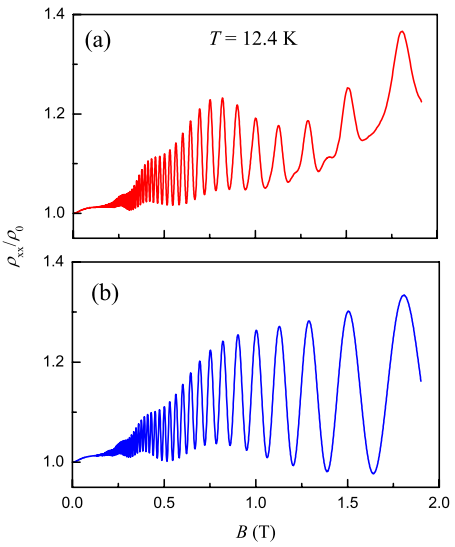

FIG. 7. (Color online) (a) Dependence of relative resistivity ρ_{xx}/ρ_0 on magnetic field. The resistance is measured in GaAs quantum well with AlAs/GaAs superlattice barriers at $T=12.4$ K. (b) Calculated dependence of the relative resistance ρ_{xx}/ρ_0 on magnetic field B. The dependence is sum of independent terms, described by Eqs. (1)–(4) and expected form of PIR oscillations.

were approximated, using similar expressions, $\Delta\rho_{\mathrm{MISO}}/\rho_0=A_{\mathrm{MISO}}\exp(-B_{\mathrm{MISO}}/B)\cos(2\pi\Delta_{12}/\hbar\omega_c)$ and $\Delta\rho_{\mathrm{PIRO}}/\rho_0=A_{\mathrm{PIRO}}\exp(-B_{\mathrm{PIRO}}/B)\cos(4\pi k_{F1}u_s/\omega_c)$.

Using the data, presented in Fig. 3(b) and Figs. 5(a) and 5(b), we determined fitting parameters. The parameters, describing the decay of the resistance oscillations, are found to be the same, $B_{QUMR}=B_{\mathrm{MISO}}=B_{\mathrm{PIRO}}=0.82$ T at $T=12.4$ K. Substitution of the value $B_{QUMR}=0.82$ T into Eq. (4) yields the quantum-scattering time $\tau_q=3$ ps. The amplitudes of different components of the relative magnetoresistance are found to be $A_{QUMR}=A_{\mathrm{MISO}}=0.28$ and $A_{\mathrm{PIRO}}=0.064$. With these fitting parameters, the calculated magnetoresistance $\rho_{xx}/\rho_0(B)$, presented in Fig. 7(b), follows well the experimental curve in a broad range of magnetic fields $B<0.7$ T. Since the fitting does not account the substantial interference between the MISO and the PIRO, the correspondence breaks at higher magnetic field. Additional analysis is required to describe quantitatively this interesting effect.

In conclusion, we have observed that the magneto-intersubband oscillations of the dissipative resistance in single GaAs quantum wells with two populated subbands coexist with the phonon-induced oscillations. The high electron mobility in the studied systems as well as the substantial difference between frequencies of these oscillations facilitates significantly the observation. These two kinds of the quantum oscillations interfere constructively. The experiments demonstrate that the enhancement of the electron-phonon scattering increases the amplitude of MISO, indicating narrowing of the intersubband resonance. We suggest that the effect is similar to the diffusive narrowing of spin resonance. The temperature suppression of the phonon-induced oscillations is found to be consistent with the broadening of the quantum electron levels and/or with the decrease in the quantum-scattering time at high temperatures. The

temperature variation in the quantum time is found to be inversely proportional to square of the temperature, indicating leading contribution of the electron-electron interaction to the decrease in the electron quantum lifetime at high temperatures.

The authors thank L. I. Magarill for useful discussion. This work was supported by RFBR under Projects No. 08-02-01051 and No. 10-02-00285 and by NSF under Grant No. DMR 0349049.

[1] H. L. Störmer, A. C. Gossard, and W. Weigmann, Solid State Commun. **41**, 707 (1982).
[2] D. R. Leadley, R. Fletcher, R. J. Nicholas, F. Tao, C. T. Foxon, and J. J. Harris, Phys. Rev. B **46**, 12439 (1992).
[3] L. I. Magarill and A. A. Romanov, Sov. Phys. Solid State **13**, 828 (1971).
[4] V. M. Polyanovskii, Sov. Phys. Semicond. **22**, 1408 (1988).
[5] M. E. Raikh and T. V. Shahbazyan, Phys. Rev. B **49**, 5531 (1994).
[6] M. A. Zudov, I. V. Ponomarev, A. L. Efros, R. R. Du, J. A. Simmons, and J. L. Reno, Phys. Rev. Lett. **86**, 3614 (2001).
[7] A. A. Bykov, A. K. Kalagin, and A. K. Bakarov, JETP Lett. **81**, 523 (2005).
[8] A. T. Hatke, M. A. Zudov, L. N. Pfeiffer, and K. W. West, Phys. Rev. Lett. **102**, 086808 (2009).
[9] A. A. Bykov and A. V. Goran, JETP Lett. **90**, 578 (2009).
[10] O. E. Raichev, Phys. Rev. B **78**, 125304 (2008).
[11] E. Zaremba, Phys. Rev. B **45**, 14143 (1992).
[12] O. E. Raichev, Phys. Rev. B **80**, 075318 (2009).
[13] K.-J. Friedland, R. Hey, H. Kostial, R. Klann, and K. Ploog, Phys. Rev. Lett. **77**, 4616 (1996).
[14] A. A. Bykov, A. K. Bakarov, L. V. Litvin, and A. I. Toropov, JETP Lett. **72**, 209 (2000).
[15] A. V. Goran, A. A. Bykov, A. I. Toropov, and S. A. Vitkalov, Phys. Rev. B **80**, 193305 (2009).
[16] N. Bloembergen, E. M. Purcell, and R. V. Pound, Phys. Rev. **73**, 679 (1948).
[17] M. E. Raikh and T. V. Shahbazyan, Phys. Rev. B **47**, 1522 (1993).
[18] E. E. Mendez, P. J. Price, and M. Heiblum, Appl. Phys. Lett. **45**, 294 (1984).
[19] J. H. English, A. C. Gossard, H. L. Stormer, and K. W. Baldwin, Appl. Phys. Lett. **50**, 1826 (1987).
[20] H. L. Stormer, L. N. Pfeiffer, K. W. Baldwin, and K. W. West, Phys. Rev. B **41**, 1278 (1990).
[21] A. V. Chaplik, Sov. Phys. JETP **33**, 997 (1971).
[22] G. F. Giuliani and J. J. Quinn, Phys. Rev. B **26**, 4421 (1982).